Available online at www.sciencedirect.com
ScienceDirect
Catalysis Today 137 (2008) 191–196
CATALYSIS TODAY
www.elsevier.com/locate/cattod

Methane activation by NO_2 on Co loaded SBA-15 catalysts: The effect of mesopores (length, diameter) on the catalytic activity

Nissrine El Hassan, Anne Davidson, Patrick Da Costa [*], Gérald Djéga-Mariadassou

Université Pierre et Marie Curie-Paris 6, UMR-CNRS 7609, Laboratoire de Réactivité de Surface, 4 place Jussieu, 75252 Paris cedex 5, France

Abstract

In a general model of ‘‘three-function deNO$_x$’’ catalyst, the partial oxidation of methane by NO_2 is an important step ($CH_4 + NO_2 \rightarrow C_xH_yO_z + NO$). To study the effect of the length and diameter, in the mesopores of SBA-15, we have synthesized catalysts with 3 wt.% cobalt supported on SBA-15, with differences in length and diameter of channels. Three different cobalt species were detected on all catalysts. We demonstrated by TPSR experiments that the activity of cobalt/SBA-15 catalysts is affected by the length, the diameter and connections between mesopores of the SBA-15 supports. We show that by changing textural properties of silica support the temperature of 100% conversion of NO_2 into NO can decrease by more than 100 °C.

Keywords: SBA-15; Cobalt; NO_2; Methane; deNO$_x$

1. Introduction

Nowadays, a major environmental problem is the selective catalytic reduction of the NO$_x$ emissions from stationary sources. Methane is one of the most convenient reductant used in this catalytic reaction because it is the principal constituent of natural gas and because the little formation of coke during the reaction.

Methane activation is the key step for the reduction of NO$_x$ by hydrocarbons. This hydrocarbon is the most difficult to activate [1]. Its activation is not possible without the presence of adsorbed species, such as $NO_{2\ \mathrm{ads}}$, which can then react with methane.

Li and Armor [2] demonstrated the activity of cobalt supported on ZSM5 zeolite catalyst for NO$_x$ removal by methane. In a general model, Djéga-Mariadassou [3] proposed that deNO$_x$ process needs three catalytic functions and concerted actions between the corresponding three catalytic cycles: (i) oxidation of NO to NO_2, (ii) mild oxidation of methane to oxidized species assisted by the reduction of NO_2 into NO and (iii) reduction of NO to N_2, assisted by the deep oxidation of the alcohol and aldehyde to CO_2. One of the challenges is to favor the second step, and thus, increase the concentration of oxygenated species that are responsible of the site regeneration in cycle 3.

The SBA-15 catalysts were never used as catalytical support for deNO$_x$ process. Thus, we prepared cobalt based catalysts supported on mesoporous silica SBA-15. These silicas were selected as supports because of their very high specific surface area (610–940 m^2/g) and their uniform pore dimension (5–8 nm in diameter) allowing the patterning of small and well calibrated oxide particles. We have used different kinds of mesoporous silica by changing the length (comparison between SBA-15 and SBA-B) or the diameter of channels (comparison between SBA-A, SBA-B and SBA-C) of these supports. The goal of this work is study the effect of lengths and diameters of pores of the support on the catalytic activity and more particularly on methane oxidation by NO_2.

2. Experimental

2.1. Catalysts preparation

All the supports were obtained using the same triblock copolymer, poly(-ethyleneoxide)-poly(-propyleneoxide)-poly(-ethyleneoxide), $EO_{20}PO_{70}EO_{20}$, kindly supplied by BASF, as a templating agent and the same molecular silica

---

[*] Corresponding author.
E-mail address: dacosta@ccr.jussieu.fr (P. Da Costa).

0920-5861/$ – see front matter © 2008 Elsevier B.V. All rights reserved.
doi:10.1016/j.cattod.2008.01.020

precursor, tetraethoxyorthosilicate (TEOS, Fluka). The SBA-15 silica used was obtained using a procedure recently reported by Choi et al. [4] with R, molar ratio between organic and inorganic species set to 45. The SBA-A, SBA-B, SBA-C and silicas were obtained using a procedure reported by Zhao et al. [5]. After preparation, SBA-B and SBA-C were submitted hydrothermal treatments for 24 h at 100 and 130 °C, respectively. Porosities of all silica have been created by calcination at 500 °C, 9 h in flowing air (100 ml min^{-1}). All samples were obtained by wet impregnation, using the porous volume of the support of aqueous 0.03 M solutions of Co nitrates for 1 g of silica. All the obtained solids were calcined at 450 °C for 5 h to fully transform nitrate precursors into oxides.

2.2. Characterisation methods

Elementary analyses were performed by inductive coupling plasma at the CNRS center of chemical analysis (Solaize, France) to determine Co and Si content. Transition electron microscopy (TEM) measurements were made with a JEOL JEM-100 CX II TEM operating at 100 keV. Samples were prepared either by dispersing the powders in a slurry of dry ethanol, deposited on a copper grid covered with a holey carbon thin film or included within a resin for the preparation of ultrathin sections of the silica grains. In the last case, a few milligrams of powder were deposited in the bottom of a Beam capsule. Some embedding resin (AGAR 100) was added and polymerized overnight at 60 °C. The polymerized blocks were cut using a diamond knife. Ultrathin sections of about 70 nm thick were recovered on copper grids. On the obtained sections presented here, silica grains are cut perpendicular to this axis (transversal). Raw HRTEM images with magnifications of 33,000 and 4,70,000 were recorded on classical 6 cm × 9 cm photographic films that were numerized using a ThetaScan UMax scanner at a resolution ranging between 800 and 1000 ppi. The N_2 sorption isotherms were measured with an ASAP 2010 apparatus (Micromeritics, Norcross, GA). Prior to the experiment, the samples were dehydrated at 250 °C for a few hours under a vacuum better than 10^{-4} Torr. A single point total pore volume was estimated circa $P/P^0 = 0.98$. The specific surface area was obtained by treating, using Brunauer, Emmett and Teller equations, for the points corresponding to P/P^0 in the range 0.05–0.25. An estimate of the average diameter of primary mesopores, labelled D_{BJH}, was derived from the maximum of the pore size distribution curve obtained by applying the Barrett, Joyner and Halenda formula to the desorption part of the isotherm, for P/P^0 greater than 0.31. This last technique of analysis is known to be incorrect in the simultaneous presence of micropores and mesopores. It underestimates mesopore diameters but relative variations among samples should be correct.

2.3. Redox properties

Temperature programmed reduction and oxidation experiments were carried out to study the nature and oxidation state of cobalt species. We have used a Micromeritics Autochem 2910 instrument equipped with a thermal conductivity detector (TCD). Data points, as TCD signals, were automatically recorded with the software Win 2910 then processed by using the software Peakfit for smoothing, baseline correction and peaks integrations. All the catalysts were pre-oxidized before reduction up to 500 °C under flowing oxygen (5% in He, 10 ml/min), at a heating rate of 10 °C/min. Reductions were performed under an H_2/Ar flow (20 ml/min), with a heating rate of 10 °C/min, up to 1000 °C.

2.4. Catalytic measurements

The catalytic reaction was performed with the following reactants: 150 ppm NO_2, 0 vol.% O_2, 0 vol.% CO_2, 1500 ppm CH_4, 0 vol.% H_2O in Ar as balance. The NO_2 mixture was supplied by Air Liquide as 5000 ppm NO_2, and 99 vol.% Ar (<10 ppm other gases). The CH_4 mixture contained 5 vol.% CH_4, and 95 vol.% Ar (Air Liquide). The total gas flow was maintained at 0.25 L min^{-1} NTP. Each gas mixture was metered using calibrated electronic mass flow controllers (Brooks, Model 5850E). Considering a catalyst density of about 0.7 g/cm^3, the gas hourly space velocity (GHSV) was 20,000 h^{-1}. Catalytic experiments were carried out in a glass microreactor (inner diameter 10 mm) containing quartz wool supporting the sample. The bed temperature was measured using a K-type thermocouple affixed to the outer reactor surface. The temperature was controlled using an electronic controller (Eurotherm 2408). The reactor outflow was analyzed using a set of specific detectors. An Eco Physics CLD 700 AL NO_x chemiluminescence analyzer for NO and total NO_x (i.e. NO + NO_2) allowed the simultaneous detection of NO, NO_2 and NO_x. An Ultramat 6 IR analyzer was used to monitor N_2O and a FID detector was used to follow the total concentration of hydrocarbons (HC). CO and CO_2 have been detected by IR detectors. Temperature programmed surface reaction (TPSR) experiments were carried out with all gases with a heating rate of 5 °C min^{-1}, up to 500 °C.

3. Discussion

3.1. Catalysts characterization

Chemical analysis data and N_2 sorption information about catalysts and parent silica supports in their blank form are presented in Table 1.

The N_2 sorption isotherms of all the samples are characteristic of materials having an uniform mesoscale porosity: they are of type IV with a H_1 hysteresis loop (figures not shown). The large specific surface area and porous volumes observed with the samples obtained stay within a range typically observed with well ordered mesoporous silicas. This confirms that the porous network is not strongly affected, neither destroyed nor partially collapsed, after the introduction of the cobalt and the calcination treatments used to generate oxide particles. Both the BET surface area and the pore volume significantly decreased upon cobalt impregnation indicating the presence of oxide particles within the porosity, as will be

Table 1
Chemical and N_2 sorption information about selected samples

	Chemical analysis Co/Si at.% ratio	N_2 sorption			
		Specific surface area[a] (m^2/g)	Porous volume[b] (cm^3/g)	ΔV_p[c] (%)	D[d] (nm)
SBA-15		868	1.1		6.0
Co/SBA-15	2.4	716	0.9	95	5.6
SBA-A		613	0.7		5.3
Co/SBA-A	3.0[e]	577	0.7	93	5.0
SBA-B		936	1.2		6.2
Co/SBA-B	3.8	631	0.7	74	6.1
SBA-C		766	1.3		8.0
Co/SBA-C	3.5	618	1.0	88	8.1

[a] Determined by applying the Brunauer, Emmett and Teller equations to the low part of the isotherm, relative pressure P/P^0 within the range 0.05–0.30.
[b] Single point, determined at $P/P^0 = 0.98$.
[c] Preserved percentage of porosity obtained from the difference between the observed volume (corrected from the mass of non porous material) and the one of the blank silica.
[d] Mesopore average diameter determined by applying the Barret, Joyner and Halenda model to the desorption branch of the isotherm.
[e] Approximative value.

observed in TEM and as we can see on the ultra thin section (A2), the cobalt oxide is located in the channels of the support SBA-15.

In TEM images, the four blank silicas powder appears composed of elongated grains (not shown). Lengths of silica grains were directly measured on TEM images. The study was done on 50 grains for each silica. 2 μm is the length of SBA-15 grains and 1 μm the length of SBA-A, SBA-B and SBA-C grains. The images depend upon the thickness of these grains and the relative orientation of their main axis and the electronic beam. When their main axis is perpendicular to the beam, alternating clear and dark stripes are observed, due to electronic density contrast between empty mesopores and silica walls. When their main axis is oriented parallel to the direction of the beam, the two dimensions hexagonal, "honey-comb", structure is revealed. The grains forming the two powders are heterogeneous both in size and shape. Representative images obtained on Co-loaded catalysts are shown in Fig. 1. Silica walls are still observed in grey whereas oxide particles, of larger electronic density, are black. Additional ultrathin sections (Fig. 1A2 and A3) reveal that these oxide particles are mainly located within the mesopores.

3.2. Catalysts redox properties tested by TPO-TPR

TPR profiles give information about the reducibility and the oxidation state of metallic species: larger oxidation state being easier to reduce and therefore giving H_2 consumption peaks at lower temperatures. The temperature at which a reduction takes place is kinetically controlled. With non-porous supports, kinetics can be affected by the size of the supported particles, the nature of support/particles interactions and the gas composition [6]. Since we have always used the same experimental conditions and since the interactions between silica and oxide particles is expected to be weak, temperature variations associated with particles sizes were mainly expected here. However, with porous supports, the situation is probably more complex. For Co-loaded MCM-41 and MCM-48 silicas, it has been postulated that water, formed during reduction steps and trapped in small pores, create diffusion hindrances for the reduction H_2 gas [7]. Three main contributions can be identified on the TPR profiles of Co-loaded catalysts based on silica [8–10]: (i) a first and relatively narrow peak around 300 °C, attributed to Co_3O_4 particles, the presence of such cobalt oxide was already confirmed by XRD (not shown in this paper) and UV–vis spectra, (ii) 1–2 broad intermediate peaks, located within the range 300–800 °C, due to Co(II) and Co(III) cations linked by Si–O–Co bonds to silica, accessible and highly dispersed and (iii) a separate peak at very high temperature, near 800–900 °C, due to poorly reducible cobalt silicates. The presence of cobalt silicate was also confirmed by IR spectra. In our experimental conditions, the three contributions are observed for the four containing cobalt samples (Fig. 2). A quantification issued from TPR experiments was also performed. The proportion of active cobalt specie is nearly identical for all catalysts. On the support without cobalt, we do not find any H_2 consumption.

3.3. Reactivity of catalysts in the activation of methane by NO_2

One of the challenges of the complete deNO_x reaction in combine heat power (CHP) is to activate the methane by the NO_2 to generate more oxidized species responsible for NO activity. This reaction corresponds to the second function of the three function catalysts model [3]. Xu et al. [11] have recently used SBA-15 based materials for N_2O decomposition. SBA-15 based materials have never been used as catalysts for SCR deNO_x applications so far. Due to the characteristics of SBA-15 silicas (very large specific surface area, well calibrated mesopore dimensions, adjustable length of silica grains), the methane activation by NO_2 could be enhanced. Then, we focused the catalytic behaviour of the prepared materials on the methane activation by NO_2.

The results are presented in Fig. 3a for the support SBA-15, and in Fig. 3b–e for samples containing cobalt. Over pure silica (SBA-15), one can see that the methane is never activated by NO_2 in the course of the reaction (Fig. 3a). However, above

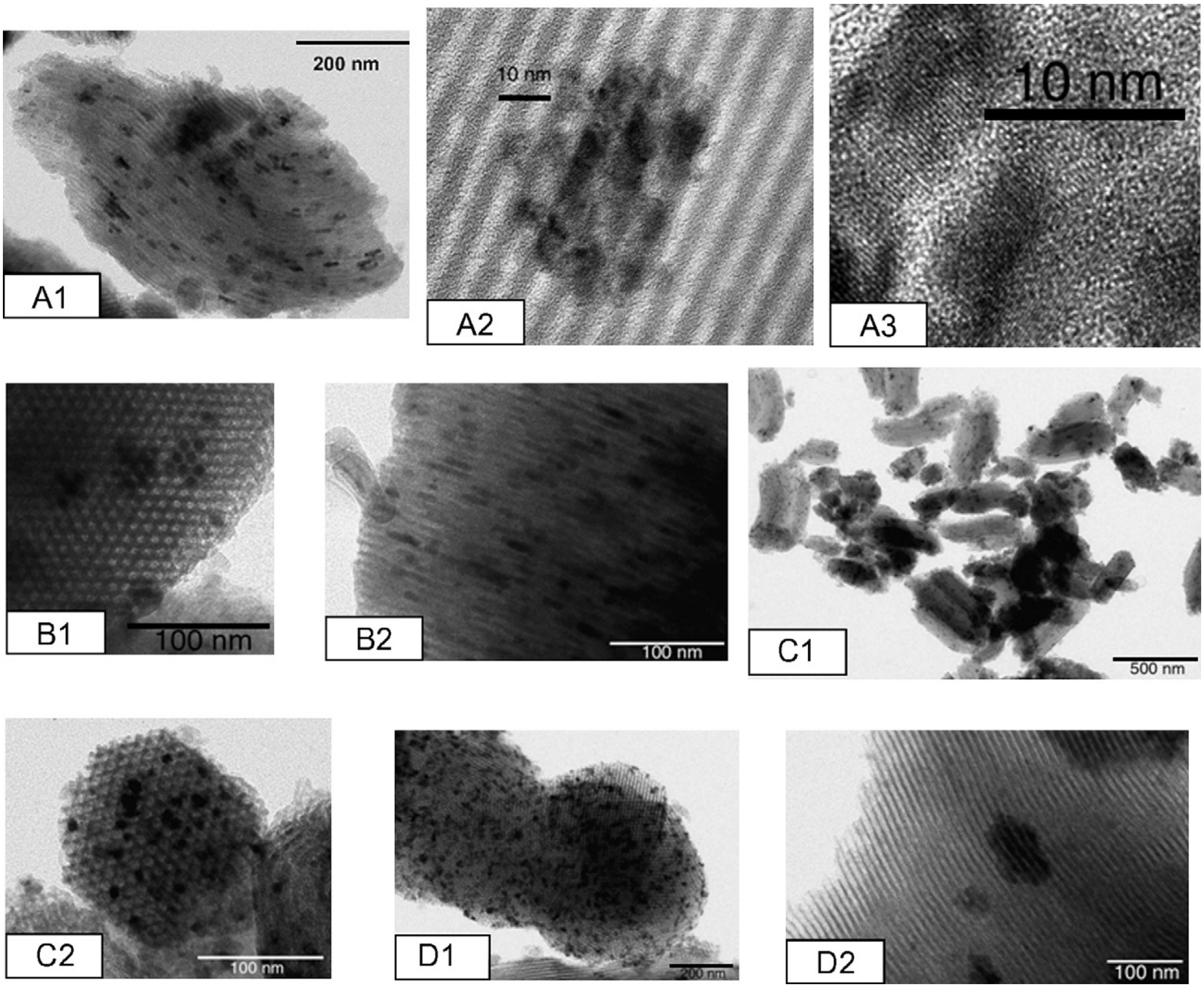

Fig. 1. TEM images of selected samples : A (1) Co/SBA-15, A (2, 3) Ultra thin section of Co/SBA-15 , B(1, 2) Co/SBA-A, C (1, 2) Co/SBA-B, D(1, 2) Co/SBA-C. Electron beam perpendicular (1) and parallel (2) to the main axis of the SBA grains Co/SBA-C.

430 °C, the reduction of NO_2 to NO takes places. When Co is present on the support, the catalytic behaviour is different. On cobalt supported SBA-15 catalysts (Fig. 3b–e), the methane is always activated – partially oxidized – at low temperature (around 130 °C) without NO_2 consumption. Methane can react on cobalt species under SBA-15 pores. Indeed, as we can see in Fig. 3b–e, the methane is adsorbed on the different cobalt SBA-15 catalysts, then desorbs between 250 and 400 °C. The results of different Co-SBA catalysts presenting different lengths and channel diameters are thus presented. The effect of length and diameter of the pores on deNO$_x$ reaction has never been reported on SBA-15. However, on zeolites based catalysts, Loughran and Resasco [12] have shown that residence time has an influence on deNO$_x$ activity. We first present in Fig. 3b the results of a cobalt based catalysts with a length of 2 μm and a diameter of 6 nm. On this catalyst (Co-SBA-15), the methane is consumed from the RT to 300 °C. Then, a production of methane or oxygenated species is observed from 300 to 380 °C. Finally, at higher temperature, the methane is consumed leading to CO_2. The NO_2 is only adsorbed at room temperature. Then, the concentration reaches its initial concentration at 80 °C. The NO_2 begins to be consumed at 250 °C, and is completely converted to NO at 340 °C. Thus, simultaneously, NO and $C_xH_yO_z$ are produced in the NO_2–CH_4 reaction. These results are in agreement with the three function model of deNO$_x$ [3].

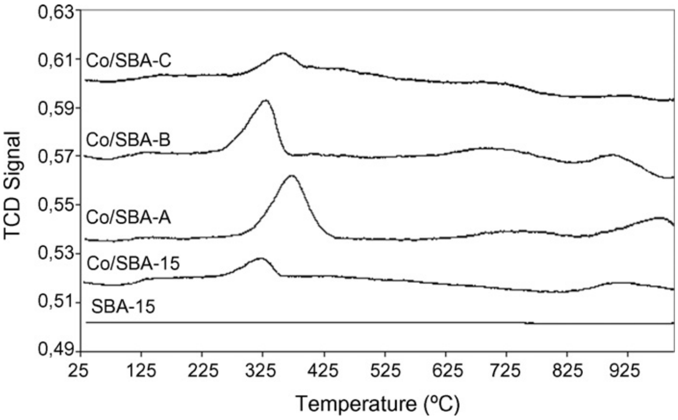

Fig. 2. TPR of selected SBA-15 support and Co-loaded on different SBA supports.

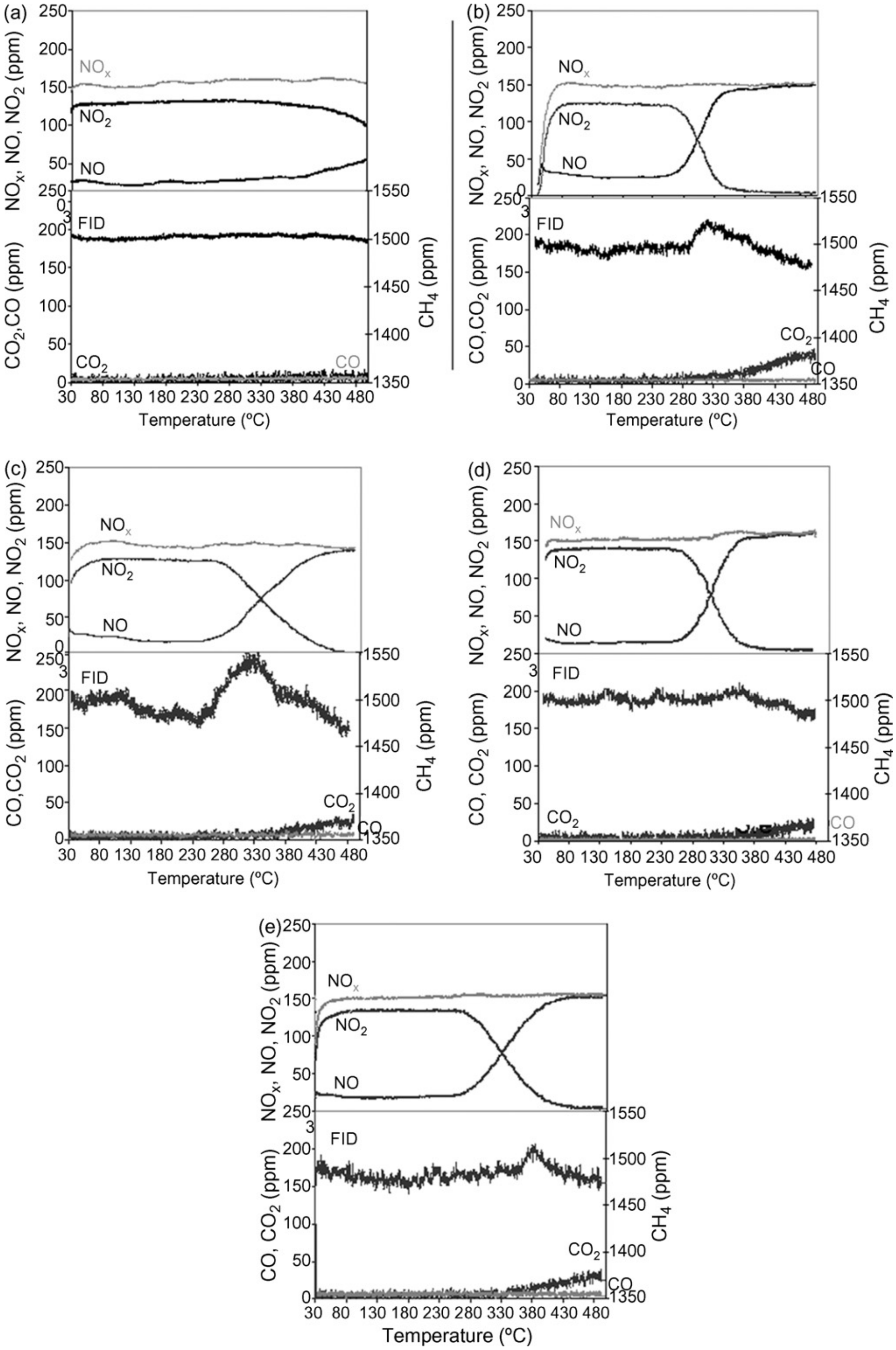

Fig. 3. (a) Temperature programmed surface reaction profiles with CH_4-NO_2 (1500 ppm–150 ppm), Ar as balance over SBA-15; (b) Temperature programmed surface reaction profiles with CH_4-NO_2 (1500 ppm–150 ppm), Ar as balance over Co/SBA-15; (c) Temperature programmed surface reaction profiles with CH_4-NO_2 (1500 ppm–150 ppm), Ar as balance over Co/SBA-B; (d) Temperature programmed surface reaction profiles with CH_4-NO_2 (1500 ppm–150 ppm), Ar as balance over Co/SBA-A; (e) Temperature programmed surface reaction profiles with CH_4-NO_2 (1500 ppm–150 ppm), Ar as balance over Co/SBA-C.

3.3.1. On the effect of SBA-15 channel length

To study the length and diameter effect, we change the catalyst in using a channel length lower than 2 μm. Thus, Co-SBA-B is used. The content of cobalt is the same, however, the length is 1 μm (Fig. 3c). In that case, the methane starts to react around 130 °C up to 280 °C. Then, a production of carbonate species such as methane or oxygenated products is observed up to 360 °C. Finally, the methane is consumed and, simultaneously, CO and CO_2 is formed. The NO_2 and NO features are similar to those observed in Fig. 3b. However, on Co-SBA-B, the NO_2 is completely converted in NO at 480 °C. If we compare the Fig. 3b and c, we can conclude that the Co-SBA-B is less active than Co-SBA-15 for NO_2–CH_4 interaction. Thus, one can conclude that the residence time which is directly proportional to the accessible mesoporous volume (as we can see in Table 1, 95% for Co-SBA-15 and 74% for Co-SBa-B), in varying the channel length from 1 to 2 μm, is important in $deNO_x$ process for NO_2–CH_4 interaction.

3.3.2. On the effect of SBA-15 pore or channel diameter

In this study, we also change the catalyst in using different pore or channel diameters. Thus, three catalysts are compared Co-SBA-B (Fig. 3c), Co-SBA-A (Fig. 3d), Co-SBA-C (Fig. 3e). For these catalysts, the content of cobalt and the length are the same (1 μm), however, the pore diameters are 6, 5 and 8 nm, respectively. The results of Co-SBA-A catalyst are presented in Fig. 3d. The activity for NO_2–CH_4 interaction begins at 265 °C. A temperature shift of 15 °C is thus observed in comparison to Co-SBA-B catalyst. Moreover, NO_2 is totally converted in NO 360 °C. As conclusion, the Co-SBA-A catalyst is more active than Co-SBA-B catalyst. This higher activity for NO_2–CH_4 reaction can be explained by a narrower way of reaction mixture in the pores of SBA-15 and thus by a higher interaction of the reactants in the support. Another catalyst (Co-SBA-C) presenting a higher pore diameter (8 nm) is also compared to Co-SBA-A and Co-SBA-B. On this catalyst (Fig. 3e), the methane reacts at the room temperature of around 350 °C, temperature at which methane or other carbonated species desorb. Simultaneously, a production of CO_2 is observed. In comparison to Co-SBA-B, the NO_2–CH_4 interaction is favoured even if the contrary was expected. For Co-SBA-C catalyst, the unexpected activity can be explained by connections existing between mesopores. These connections lead to a higher residence time of the $NO_2 + CH_4$ in this catalyst in comparison to Co-SBA-B. These connections are already presented by Galarneau et al. [13]. Finally, in terms of NO_2–CH_4 interaction, the ranking is the following:

$$\text{Co-SBA-15} = \text{Co-SBA-A} > \text{Co-SBA-C} > \text{Co-SBA-B}.$$

Thus, the size of mesopores is an important parameter in the $deNO_x$ process and more particularly in partial oxidation of methane by NO_2, (function 2 of $deNO_x$ mechanism [3]) leading to NO and oxygenated species, that are the ‘‘real reductants’’ during the NO dissociation process function 3 of $deNO_x$ mechanism [3]). The residence time is proportional to the variation of accessible mesoporous volume.

4. Conclusion

We have synthesised cobalt supported on mesoporous silica catalysts which can activate methane by NO_2. Three species of cobalt are presented for all catalysts, Co_3O_4, isolated CoO and cobalt silicate. By changing the support characteristics (length and channel diameter) we compared the activity in this type of reaction. From these results, we can conclude that when the length of SBA-15 support increases, the more activity increases. Another important point is the variation of accessible mesoporous volume. For higher ΔV_p, activity is better. Moreover, concerning the channel diameter, we can observe that when the diameter decreases (comparison between Co/SBA-A [5 nm] and Co/-SBA-B [6 nm]), the contact between reactants increase (the smaller the space between us, the more the contact) and the activity of the catalyst increases. This argument changes if we look at the two catalysts, Co-SBA-B [6 nm] and Co-SBA-C [8 nm]. For the support SBA-C, some connections between mesopores are present. Thus, the residence time increases in comparison to SBA-B. So the activity for Co-SBA-C is better than those of Co-SBA-B.

References

[1] R. Burch, M.J. Hayes, J. Mol. Catal. A 100 (1995) 13.
[2] Y. Li, J.N. Armor, Appl. Catal. B 1 (4) (1992) L31.
[3] G. Djéga-Mariadassou, Catal. Today 90 (2004) 27.
[4] M. Choi, W. Heo, F. Kleitz, R. Ryoo, Chem. Commun. (2003) 1340.
[5] D. Zhao, J. Feng, Q. Huo, N. Melosh, G.H. Fredrickson, B.F. Chmelka, G.D. Stucky, Science 279 (1998) 548.
[6] B. Jongsomjit, J. Panpranot, J.G.J. Goodwin, Catal. Today 204 (2001) 98.
[7] T. Vralstad, W.R. Glomm, G. Oye, J. Sjoblom, M. Stocker, J. Dispos. Sci. Tech. 26 (2005) 87.
[8] Y. Okamoto, K. Nagata, T. Adichi, T. Imanaka, K. Inamura, T. Takyu, J. Phys. Chem. 95 (1991) 310.
[9] E.V. Steen, G.S. Sewell, R.A. Makhothe, C. Mickelethwaite, H. Manstein, M. de Lange, C.T. O’Connor, J. Catal. 162 (1996) 220.
[10] I. Puskas, T.H. Fleisch, J.B. Hall, B.L. Meyers, R.T. Roginski, J. Catal. 134 (1992) 615.
[11] X. Xu, H. Xu, F. Kapteijn, J.A. Moulijn, Appl. Catal. B 53 (2004) 265.
[12] C.J. Loughran, D.E. Resasco, Appl. Catal. B 7 (1995) 113.
[13] A. Galarneau, H. Cambon, F. Di Renzo, R. Ryoo, M. Choi, F. Fajula, New J. Chem. 27 (2003) 73.